British Journal of Applied Science & Technology
14(3): 1-8, 2016, Article no.BJAST.23602
ISSN: 2231-0843, NLM ID: 101664541

SCIENCEDOMAIN *international*
www.sciencedomain.org

On Influence of Aspect Ratio on Jamming Probability for Flows of Elliptical Disks in a Two-dimensional Rotating Hopper

Yung-Jung Lin[1], Chung Fang[1*] and Chin-Wan Chen[1]

[1]Department of Civil Engineering, National Cheng Kung University, No.1, University Road, Tainan City 701, Taiwan.

Authors' contributions

This work was carried out in collaboration between all authors. Author CF designed the study, performed the statistical analysis, wrote the protocol, wrote the first draft of the manuscript and managed literature searches. Authors YJL and CWC managed the analyses of the study and literature searches. All authors read and approved the final manuscript.

Article Information

DOI: 10.9734/BJAST/2016/23602
Editor(s):
(1) Elena Lanchares Sancho, Department of Mechanical Engineering, University of Zaragoza, Zaragoza, Spain.
(2) Singiresu S. Rao, Prof. at Department of Mechanical and Aerospace Engineering, University of Miami, Coral Gables, USA.
Reviewers:
(1) Siva Prasad Kondapalli, Anil Neerukonda Institute of Technology & Sciences, India.
(2) Anonymous, University of Malaya, Malaysia.
(3) Zhi Shang, Louisiana State University, USA.
Complete Peer review History: http://sciencedomain.org/review-history/13144

Original Research Article

Received 9th December 2015
Accepted 26th January 2016
Published 3rd February 2016

ABSTRACT

Jamming arches and jamming probability of flowing elliptical disks at the opening of a two-dimensional rotating hopper is studied experimentally. A two-dimensional rotating hopper of Plexiglas with variable opening width and slope is constructed to conduct quasi two-dimensional flows of elliptical disks with different aspect ratios. Results show that the jamming probability and jamming arch structures are significantly influenced by the aspect ratio. There exist an upper and a lower limit of the hopper opening width, in which the jamming probability decreases monotonically as the opening width increases. When the opening is smaller than the lower limit, completely jamming takes place, while above the upper limit no jamming appears. As the aspect ratio increases, the jamming probability increases correspondingly for fixed hopper slope and opening width. For the jamming arch structures, increasing the aspect ratio tends to induce smaller horizontal average span, with a fluctuating tendency of the vertical average span for fixed values of

**Corresponding author: E-mail: cfang@mail.ncku.edu.tw;*

the average arch number. For a fixed horizontal average span, increasing the aspect ratio gives rise to increase the average arch number. These imply that, for less narrow disks, the induced jamming arches are more semi-circular, while relatively flat jamming arches are triggered when disks are more narrow. The study delivers a physical mechanism of jamming phenomena of elliptical disks in a two-dimensional rotating hopper.

Keywords: Elliptical disks; jamming arches; jamming probability; rotating hopper.

1. INTRODUCTION

Dry granular matter is of a large amount of discrete solid grains, in which the interstitial space is filled by a gas [1-4]. When in flows, long-term frictional contact and sliding, and short-term instantaneous inelastic collision among the grains emerge. Two-fold grain-grain interactions result in significant rheological features with distinct microstructural effects [2,4]. It happens frequently that grains accumulate themselves near the critical flow regions, at which stable and unstable force chains in arches are induced, transiting fluid-like motion to solid-like state [1,5,6]. While stable arches are sufficient to halt the impact of the incoming grains to jam the flow, unstable arches may be broken, yielding typical stick-slip phenomena [1,4,7,8]. This may induce unexpected pressure fluctuations on the side walls of hoppers and silos, and lead to not only unfavorable discontinuous mass discharge flows, but also trigger, in most serious circumstances, failure of the storage facilities [1,3,4]. Thus, the jamming arches near the throat regions of hopper and silo flow passages need to be investigated to avoid unfavorable structure failure in discharging processes of dry granular raw material or products.

Jamming near the openings of hoppers and silos has been studied experimentally for dry spherical grains, e.g. [9-16]. The grain size (grain diameter), hopper flow passage slope and opening were recognized to be critical in jamming processes. The jamming probability decreased exponentially as the dimensionless opening increased [13-16]. There existed a critical dimensionless opening, over which arches could not be formed. However, the relation between jamming probability and grain geometry was yet clear [17,18]. Simulations by using Discrete Element Method (DEM), based on hard- and soft-sphere models, have been conducted, with simulated results similar to those of experimental outcomes for spherical grains, e.g. [19-23]. For non-spherical grains, due to that the contact points and force chains were hardly determined, the simplification of non-rotating grains yielded unsatisfactory outcomes. Theoretical studies on arch structures were essentially based on the restricted self-avoiding random walker model and statistical mechanics for spherical grains, e.g. [13-16], while extensions for non-spherical grains seemed inappropriate.

Jamming probability was equally influenced by the grain properties and arrangements for spherical grains, e.g. [21-26]. Increasing grain amount in a two-dimensional rotating hopper tended to increase jamming probability for fixed hopper slope and opening, while reducing jamming probabilities were obtained for more elastic grains, resulted from the broken of arches by more intensive momentum of the incoming grains.

Although stable arches take place more easily in non-spherical grains via the point contacts among the grains and solid boundaries, quantitative experimental studies on the influence of grain geometry on jamming processes are insufficient. The focus of the study is thus on the influence of grain geometry on jamming probability in hopper and silo flows. Specifically, a two-dimensional rotating hopper of Plexiglas with varied slope and opening is constructed, into which elliptical Plexiglas disks with varied aspect ratios are deposited to conduct jamming processes induced by arches. The influence of the aspect ratio of the elliptical disks on the jamming probability and the corresponding jamming arches are investigated experimentally. It will be shown that there exist an upper and a lower limits of the hopper opening width, in which the jamming probability decreases monotonically as the hopper opening increases. When the opening is smaller than the lower limit, completely jamming takes place, while above the upper limit no jamming occurs. As the aspect ratio increases, the jamming probability increases correspondingly for fixed hopper slope and opening width. For less narrow disks, the induced jamming arches are more semi-circular, while relatively flat jamming arches

are triggered when disks are more narrow. Both jamming arch structures are sufficient to halt the impact of the incoming disks to trigger jamming process.

In Sect. 2, the experimental setup and procedure are outlined, followed by the experimental outcomes and discussions in Sect. 3. The paper is summarized in Sect. 4.

2. EXPERIMENTAL SETUP

2.1 Two-dimensional Rotating Hopper

A two-dimensional rotating hopper is constructed, as shown in Fig. 1(a). It consists of three layers: the steel back layer, serving as the base of the hopper; the intermediate Plexiglas layers, conducting hopper flow passage; and the Plexiglas front layer, providing a confinement to the flow passage. While the back and front layers are fixed, different intermediate layers are used to accomplish two-dimensional flow passages with different hopper slopes and openings. The two-dimensional hopper integration (item 4) is attached to a steel rotating shaft (item 2), which is connected subsequently to a program-controlled servo-step motor (item 3) through a gear box to control the rotating speed and angle. The whole facility sits on a steel rigid foundation (item 1), associated with adjustable standers to maintain water level and minimize mechanical vibration during experiments. The overall dimensions of the experimental facility are shown in Fig. 1(a). Specifically, the thickness of the intermediate layers is slightly larger than that of elliptical disks to prevent particle overlapping during flows. With these, quasi two-dimensional hopper flows can be approximated.

2.2 Elliptical Disks

Two-dimensional elliptical disks of different aspect ratios, *e* = [1.0, 1.5, 2.0, 2.5, 3.0], are made of Plexiglas, shown in Figs. 1(b) and 1(c). The disk surfaces correspond to that of a spherical disk with a diameter of 5 mm. This is done so to minimize the influence of particle size segregation [1-4]. The disk thickness is 2 mm, slightly smaller than that of the hopper flow passage. The disks are polished to minimize contact friction among disks and solid boundaries. The dimensions of the two-dimensional rotating hopper facility and elliptical disks are summarized in Table 1.

Table 1. Dimensions of the two-dimensional rotating hopper and elliptical disks

Two-dimensional hopper facility	
Facility overall height	~ 1160 mm
Facility overall width	~ 760 mm
Facility overall depth	~ 950 mm
Height of the hopper integration	900 mm
Width of the hopper integration	520 mm
Thickness of the hopper integration	13 mm
Thickness of the back layer	5mm (steel plate)
Thickness of the intermediate layers	3 mm (Plexiglas plate)
Thickness of the front layer	5 mm (Plexiglas plate)
Elliptical disks	
Thickness	2 mm
Aspect ratio	1.0, 1.5, 2.0, 2.5, 3.0

2.3 Theoretical Basis

For spherical disks, the typical jamming arches are shown schematically in Fig. 2. The jamming probability can be approximated by using the restricted self-avoiding random walker model [13-16], with the following geometric restrictions assumed a priori:

$$\frac{\pi}{2} > \theta_i > -\frac{\pi}{2}; \quad \theta_1 > \cdots > \theta_i > \theta_{n-1};$$
$$\left| \sum_{k=1}^{i} r_k - \sum_{k=1}^{i} r_k \right| \geq D, \quad \forall i \neq j; \tag{1}$$

in which r_i denotes the straight line from the center of the i^{th} disk toward that of the $i+1^{th}$ disk, θ_i is the inclined angle of r_i with respect to the horizontal line, and *D* is the disk diameter. In doing so, the jamming arch is assumed to consist of *n* spherical disks. While the above geometric restrictions are appropriate for spherical disks, for the force chain exists along the lines connecting the centers of the disks, they are not applicable for non-spherical disks. This is due to that during flows the non-spherical disks may experience significant rotations, yielding complex distributions of the contact points among the disks. As to our knowledge, theoretical analysis of jamming arches of non-spherical disks is yet completed. Thus, the focus of the study is to investigate the jamming arches and resulting jamming probability of elliptical disks in a two-dimensional rotating hopper by using experiments.

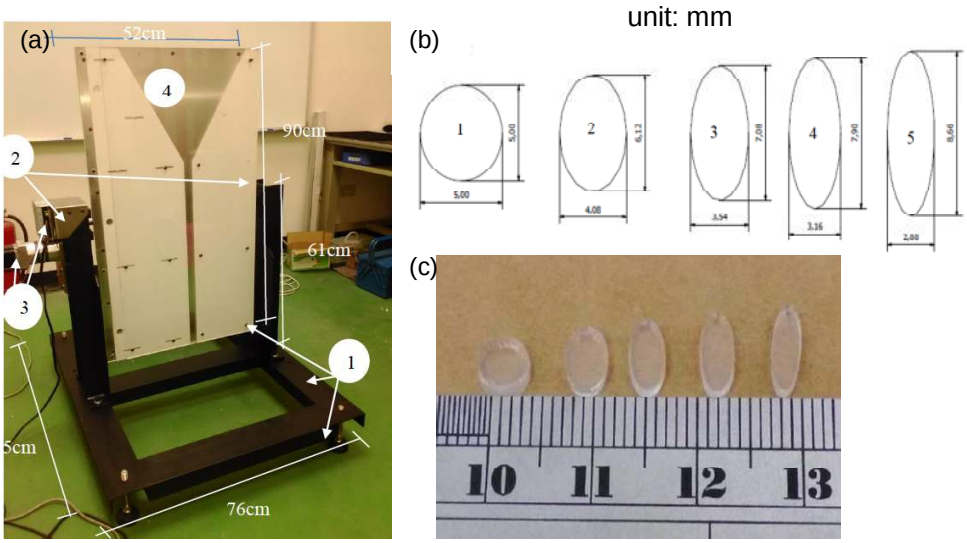

Fig. 1. (a) Two-dimensional rotating hopper with overall dimensions; (b) Schematic illustration of the elliptical disks (unit: mm); (c) Prototype of the elliptical disks of Plexiglas

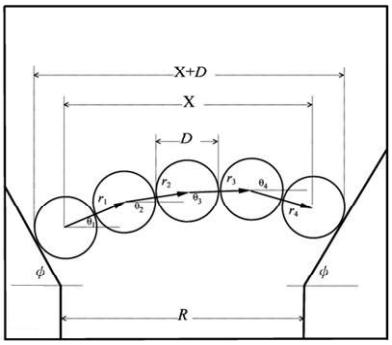

Fig. 2. Typical jamming arch of spherical disks in a two-dimensional hopper [13]

2.4 Experimental Procedure

In experiments, the hopper slope is fixed, while the hopper opening and aspect ratio of the elliptical disks are considered controlled parameters, with the experimental setup summarized in Table 2. A fixed amount of 400 disks is confined in a rectangular slot (150 mm * 65 mm) with random orientations of the longer axes. The slot is put into the hopper, followed by the removal of the slot to conduct initial configurations of the elliptical disks. The two-dimensional hopper is rotated from horizontal position to completely vertical position (i.e., 90° rotating angle) in a fixed time duration to conduct two-dimensional hopper flows of elliptical disks. In each setup of the controlled parameters, 50 times experiments are conducted to determine the jamming probability P_J defined by

$$P_J \equiv \frac{N_J}{N}; \quad \bar{d} = \frac{d}{a_s}, \tag{2}$$

with N_J the number of jammed flows and N the total number of experiments (i.e., N = 50). In equation $(2)_2$, $\bar{d}$ is the dimensionless hopper opening, with a_s the shorter axis dimensions of elliptical disks. It is used in the forthcoming analyses to illustrate the jamming probability. In addition, the following three parameters are defined:

$$n_A = \frac{n_J}{N_J}; \ \bar{x}_s = \frac{x_s}{N_J}, \ \ \bar{y}_s = \frac{y_s}{N_J}, \tag{3}$$

where n_A is the average arch number, n_J the disk number consisting of jamming arch, $\bar{x}_s$ the average x-span of jamming arches, $\bar{y}_s$ the average y-span of jamming arches, and x_s and y_s the horizontal and vertical spans of the jamming arches, respectively. These parameters are used to distinguish the structures of jamming arches.

Table 2. Setup of jamming experiments

Hopper slope	$\theta = 60°$ (fixed)
Amount of elliptical disks	400 (fixed)
Time duration of 90 degree rotation	30 s (fixed)
Hopper opening width	$d = 10\sim30$ mm (varied)
Aspect ratio of elliptical disks	$e = 1.0, 1.5, 2.0, 2.5, 3.0$ (varied)

3. EXPERIMENTAL OUTCOMES AND DISCUSSION

3.1 Experimental Calibration

Fig. 3(a) shows the distribution of P_J versus $\bar{d}$ for the hopper slope of $\theta = 60°$ for spherical disks; dotted line: the experimental outcome by using the constructed facility; data points: experimental outcomes quoted from [13,14], in which square, triangle and diamond points correspond to the 200-, 400- and 700-disks, respectively. The dotted line demonstrates a nearly similar tendency as the experimental data points. There exist an upper and a lower limits of $\bar{d}$. Complete jamming takes place when $\bar{d}$ is smaller than its lower limit, while no jamming appears when $\bar{d}$ is larger than its upper limit. In-between P_J decreases nearly exponentially as $\bar{d}$ increases. The discrepancy between the dotted line and data points corresponding to 400-disks results from that (1) different spherical disks are used (dotted line: disks of Plexiglas; data points: disks of aluminum), and (2) the hopper rotating speeds are different. However, Fig. 3(a) delivers that P_J estimated by using the constructed facility is similar to those of other experimental outcomes, and provides a calibration of the experimental setup in the study.

3.2 Influence of Aspect Ratio and Hopper Opening

The influence of $\bar{d}$ on P_J is shown in Fig. 3(b), in which the amount of disks is 400, $\theta = 60°$ and e = [1.0, 1.5, 2.0, 2.5, 3.0], indicated by the arrow. For fixed values of e, there exist an upper and a lower limits of $\bar{d}$. When the hopper opening is smaller than the lower limit, flows are completely jammed, giving rise to an unity jamming probability. When the hopper opening is larger than the upper limit, no jammed flows are recognized. In-between, P_J decreases exponentially as $\bar{d}$ increases. Similar tendencies are manifest for different values of e. Specifically, as e increases, the upper and lower limits of $\bar{d}$ shift gradually to the right, implying that for more narrow disks, smaller hopper opening can trigger stable jamming arches to yield jamming, while larger hopper opening is necessary for jamming. Similarly, as the aspect ratio increases, the jamming probability increases correspondingly. This results from that for more narrow disks, the disks can travel longer distances with significant rotations, so that force chains can be induced through the contacts near the narrow regions among the disks and solid boundaries. The induced force chains are relatively strong, and are sufficient to sustain the impacts of the incoming disks to induce jamming, giving rise to larger jamming probability.

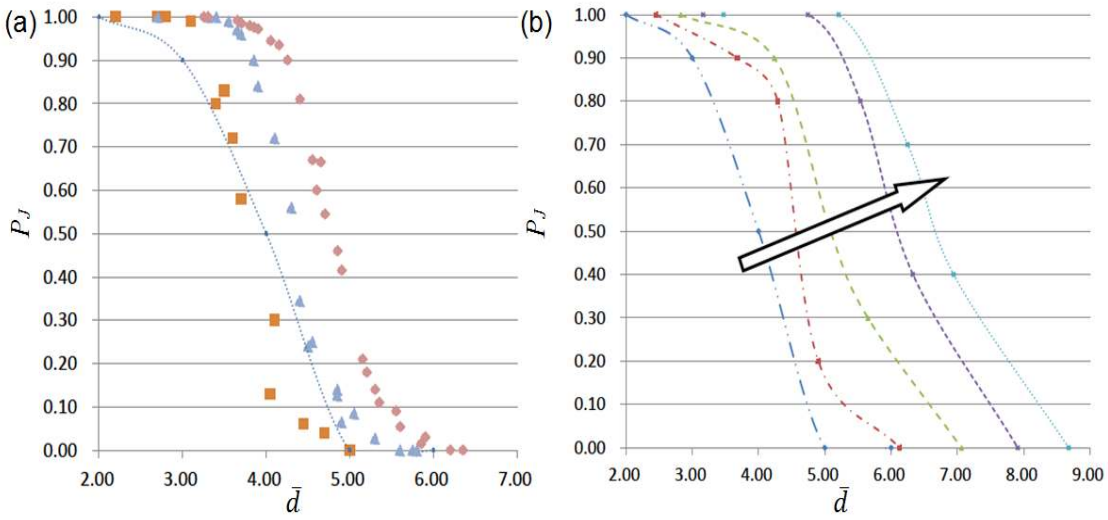

Fig. 3. Jamming probability versus hopper opening width

(a) Experimental calibration for spherical disks; experimental data quoted from [13,14], in which square points correspond to the amount of 200 disks, triangle and diamond points correspond to the amounts of 400 and 700 disks, respectively. (b) Experimental outcomes of jamming probability on variations in e = [1.0, 1.5, 2.0, 2.5, 3.0] indicated by the arrow for 400 disks

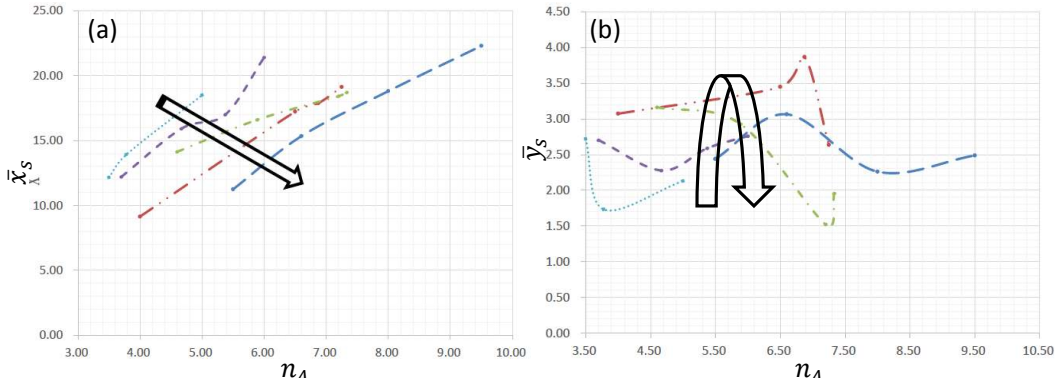

Fig. 4. Jamming arch structures

(a) Average x-span, $\bar{x}_s$, in relation with the average arch number, n_A. (b) Average y-span, $\bar{y}_s$, in relation with the average arch number, n_A, in which e = [1.0, 1.5, 2.0, 2.5, 3.0] indicated by the arrows. Dotted lines: e = 1.0; short dashed lines: e = 1.5; dashed-dotted lines: e = 2.0; dashed-doubled-dotted lines: e = 2.5; long dashed lines: e = 3.0. The amount of disks: 400

3.3 Structures of Jamming Arches

Figs. 4(a) and 4(b) illustrate the analyses of the typical jamming arch structures for the amount of 400 disks, $\theta = 60°$ and variations in *e* = [1.0, 1.5, 2.0, 2.5, 3.0], indicated by the arrows, in terms of the average arch number n_A versus the average *x*-span, $\bar{x}_s$, and *y*-span, $\bar{y}_s$, respectively. For spherical disks (*e* = 1.0), a certain amount of disks is needed to form stable semi-circular arches, in which force chains align to the centers among the disks (dotted lines). As *e* increases, the number of disks consisting of jamming arches, n_A, increases correspondingly, implying that stable jamming arches can be induced in a distance away from the hopper opening. Based on this, more disks are required to form stable semi-circular jamming arches. However, larger values of *e* tend to yield larger values of n_A (e.g. dashed line), implying that for more narrow disks, stable jamming arches can be formed in the neighboring regions near the hopper opening, in which jamming arches become less semi-circular. Such a tendency is also revealed by the increasing tendency of the relations between $\bar{x}_s$ and n_A for different values of *e*, as shown in Fig. 4(a). This is due to that for more narrow disks, the disks are traveling longer distance with significant rotations, by which their longer axes are aligning toward the hopper opening. At the neighboring locations near the hopper opening, relatively flat stable jamming arches can be formed through the strong contacts among the narrow parts of the disks, giving rise to larger jamming probability, as already demonstrated in Fig. 3.

More precise jamming arch structures can be recognized by the $\bar{y}_s$-distributions, as shown in Fig. 4(b). For fixed values of *e*, $\bar{y}_s$ increases gradually for smaller values of n_A, while it drops for larger values of n_A. Similar tendencies are manifest for different values of *e*. However, $\bar{y}_s$ experiences fluctuations as *e* increases. This reflects that for less narrow disks, the induced stable jamming arches are nearly semi-circular, while for more narrow disks, relatively flat jamming arches are sufficient to trigger jamming. The tendency is equally indicated by the fluctuating tendencies of the relations between $\bar{y}_s$ and n_A as *e* increases. The results correspond nearly to those recognized in a two-dimensional static hopper [27].

4. CONCLUDING REMARKS

A two-dimensional rotating hopper of Plexiglas, driven by program-controlled servo-step motor, was constructed to conduct quasi two-dimensional hopper flows of elliptical disks, which were made of Plexiglas with different aspect ratios. The disks were deposited into the hopper to conduct two-dimensional hopper flows of elliptical disks, for which the jamming probability, jamming arch structures and influence of hopper opening and aspect ratio of the disks were investigated experimentally.

In contrast to the jamming processes in a static hopper, in which the disks experience constant gravity, the disks in the rotating hopper experience increasing gravity, in which the jamming is significantly influenced by the disk-disk and disk-boundary interactions. It is found

that for fixed hopper slope, opening width and aspect ratio, there exist an upper and a lower limits of the dimensionless hopper opening. Below the lower limit flows are completely jammed, giving rise to an unity jamming probability; while above the upper limit no jammed flows take place. In-between the jamming probability decreases exponentially as the dimensionless hopper opening increases. The jamming probability increases correspondingly as the aspect ratio increases. For less narrow disks, the number of disks consisting of jamming arches increases correspondingly, implying that stable jamming arches with larger amounts of disks, possibly in relatively semi-circular forms, can be formed in a distance away from the hopper opening. On the contrary, for more narrow disks, stable jamming arches can be formed in the neighboring regions near the hopper opening, in which jamming arches become less semi-circular with smaller amounts of disks. The force chains in the jamming arches are induced through the strong point contacts among the narrow parts of the disks, which are sufficient to halt the momentum of the incoming disks to give rise to larger jamming probability.

ACKNOWLEDGEMENTS

The authors are indebted to the Ministry of Science and Technology, Taiwan, for the financial support via the project NSC 102-2221-E-006-198-. The authors thank the editor and reviewers for the suggestions and comments which led to improvements.

COMPETING INTERESTS

Authors have declared that no competing interests exist.

REFERENCES

1. Aranson IS, Tsimring LS. Granular patterns. Oxford University Press, Oxford; 2009.
2. Ausloos M, Lambiotte R, Trojan K, Koza Z, Pekala M. Granular matter: A wonderful world of clusters in far-from-equilibrium systems. Physica A. 2005;357:337-349.
3. Poschel T, Brilliantov NV. Granular gas dynamics, In: Lecture Notes in Physics (Book 624), Springer-Verlag, New York; 2013.
4. Rao KK, Nott PR. An introduction to granular flow. Cambridge University Press, Cambridge; 2008.
5. Fang C. Rheological characteristics of solid-fluid transition in dry granular dense flows: A thermodynamically consistent constitutive model with a pressure-ratio order parameter. International Journal for Numerical and Analytical Methods in Geomechanics. 2010;34:881-905.
6. Fang C. Gravity-driven dry granular slow flows down an inclined moving plane: A comparative study between two concepts of the evolution of porosity. Rheologica Acta. 2009;48:971-992.
7. Hoang TH. Frottement saccad_e dans les mat_eriaux granularies mod_eles, PhD Thesis, L'Institut National des Sciences Appliqu_ees de Lyon, France; 2011.
8. Doanh T, Hoang MT, Roux J-N, Dequeker C. Stick-slip behavior of model granular materials in drained tri-axial compression. Granular Matter. 2013;15:1-23.
9. Garcimartín A, Zuriguel I, Pugnaloni LA, Janda A. Shape of jamming arches in two-dimensional deposits of granular materials. Physical Review E. 2010;82:031306.
10. Janda A, Zuriguel I, Garcimartín A, Pugnaloni LA, Maza D. Jamming and critical outlet size in the discharge of a two-dimensional silo. Europhysics Letters. 2008;84:44002.
11. Janda A, Harich R, Zuriguel I, Maza D, Cixous P, Garcimartín A. Flow-rate fluctuations in the outpouring of grains from a two-dimensional silo. Physical Review E. 2009;79:031302.
12. Magalhães CFM, Moreira JG, Atman APF. Catastrophic regime in the discharge of a granular pile. Physical Review E. 2010; 82:051303.
13. To K, Lai PY, Pak HK. Jamming of granular flow in a two-dimensional hopper. Physical Review Letters. 2001;86:71-74.
14. To K. Jamming transition in two-dimensional hoppers and silos. Physical Review E. 2005;71:060301.
15. Sheldon HG, Durian DJ. Granular discharge and clogging for tilted hoppers. Granular Matter. 2010;12:579-585.
16. To K, Lai PY, Pak HK. Flow and jam of granular particles in a two-dimensional hopper. Physica A: Statistical Mechanics and its Applications. 2002;315:174-180.
17. Jin BS, Tao H, Zhong WQ. Flow behaviors of non-spherical granules in rectangular

hopper. Chinese Journal of Chemical Engineering. 2010;18:931-939.
18. Mack S, Langston P, Webb C, York T. Experimental validation of polyhedral discrete element model. Powder Technology. 2011;214:431-442.
19. Balevičius R, Kačianauskas R, Mróz Z, Sielamowicz I. Analysis and DEM simulation of granular material flow patterns in hopper models of different shapes. Advanced Powder Technology. 2011;22:226-235.
20. Tao H, Jin BS, Zhong WQ, Wang XF, Ren B, Zhang Y, Xiao R. Discrete element method modeling of non-spherical granular flow in rectangular hopper. Chemical Engineering and Processing: Process Intensification. 2010;49:151-158.
21. Wang J, Yu HS, Langston P, Fraige F. Particle shape effects in discrete element modeling of cohesive angular particles. Granular Matter. 2011;13:1-12.
22. Fraige FY, Langston PA, Matchett AJ, Dodds J. Vibration induced flow in hoppers: DEM 2D polygon model. Particuology. 2008;6;455-466.
23. Tao H, Jin BS, Zhong WQ. Simulation of ellipsoidal particle flow in rectangular hopper with discrete element method. In Electric Technology and Civil Engineering (ICETCE), 2011 International Conference on. 2011;678-681.
24. Longjas A, Monterola C, Saloma C. Force analysis of jamming with disks of different sizes in a two-dimensional hopper. Journal of Statistical Mechanics: Theory and Experiment. 2009;P05006.
25. Frank GA, Dorso CO. Room evacuation in the presence of an obstacle. Physica A: Statistical Mechanics and its Applications. 2011;390:2135-2145.
26. Saraf S, Franklin SV. Power law flow statistics in anisometric (wedge) hoppers. Physical Review E. 2011;83:030301.
27. Lin Y-J, Fang C. Experimental study on depositing arch jamming of elliptical disks in a two-dimensional static hopper. Journal of Mechanics (in press); 2016.

Peer-review history:
The peer review history for this paper can be accessed here:
http://sciencedomain.org/review-history/13144